Charged Polarons and Molecules in a Bose-Einstein Condensate

Esben Rohan Christensen,[1] Arturo Camacho-Guardian,[2,1] and Georg M. Bruun[1,3]
[1]Center for Complex Quantum Systems, Department of Physics and Astronomy, Aarhus University, Ny Munkegade 120, DK-8000 Aarhus C, Denmark
[2]T.C.M. Group, Cavendish Laboratory, University of Cambridge, JJ Thomson Avenue, Cambridge CB3 0HE, United Kingdom
[3]Shenzhen Institute for Quantum Science and Engineering and Department of Physics, Southern University of Science and Technology, Shenzhen 518055, China

(Received 29 December 2020; accepted 20 May 2021; published 16 June 2021)

Ultracold hybrid ion-atom gases represent an exciting frontier for quantum simulation offering a new set of functionalities and control. Here, we study a mobile ion immersed in a Bose-Einstein condensate and show that the long-range nature of the ion-atom interaction gives rise to an intricate interplay between few- and many-body physics. This leads to the existence of several polaronic and molecular states due to the binding of an increasing number of bosons to the ion, which is well beyond what can be described by a short-range pseudopotential. We use a complementary set of techniques including a variational ansatz and field theory to describe this rich physics and calculate the full spectral response of the ion. It follows from thermodynamic arguments that the ion-atom interaction leads to a mesoscopic dressing cloud of the polarons, and a simplified model demonstrates that the spectral weight of the molecules scale with increasing powers of the density. We finally calculate the quantum dynamics of the ion after a quench experiment.

DOI: 10.1103/PhysRevLett.126.243001

The versatility and control of atomic gases make them powerful platforms for quantum simulation of many-body systems [1,2]. Ions immersed in atomic gases represent an exciting new research direction due to their hybrid nature, which enables new functionalities and broader simulation capabilities. In particular, the excellent control of the motional and internal degrees of individual ions opens up new opportunities to explore the interaction between a small quantum system and its environment, and to address fundamental questions regarding cooling, decoherence, and entanglement. The ion can also act as a local probe, which has indeed already been exploited in classic experiments investigating vortices [3] and the properties of superfluid liquid ^{4}He [4–6] and ^{3}He [7–11].

Experiments on ions in atomic gases have explored atom-ion collisions, sympathetic cooling, controlled chemistry [12–19], transport [20], and molecular formation [21]. Theoretically, the Fröhlich model, valid for weak ion-atom interaction, was used to explore an ion in an atomic Bose-Einstein condensate (BEC) [22] and three-body recombination dynamics was studied in Refs. [23,24]. Several papers have predicted the formation of molecular ions based on kinetic and mean-field approaches [25,26], quantum defect theory [23], and time-dependent Hartree and Monte Carlo calculations [27,28].

Inspired by this exciting development, we investigate the spectral and dynamical properties of a mobile ion immersed in a BEC. We demonstrate that when the range of the ion-atom interaction is comparable to the interparticle distance, a rich interplay between few- and many-body physics arises with several polaronic and molecular states, which cannot be captured with a pseudopotential approach. Using a variational wave function that allows for the dressing of the ion by an infinite number of Bogoliubov modes, we calculate the full spectral response of the ion, and a comparison with a field theory calculation based on the Bethe-Salpeter equation demonstrates that the molecules are formed by binding an increasing number of bosons to the ion. We show using a heuristic model that the spectral weight of these molecules scale with increasing powers of the BEC density, and from thermodynamic arguments we conclude that the long-range ion-atom interaction gives rise to a mesoscopic dressing cloud of the polarons. The quantum dynamics of the ion ensuing a quench experiment unveils the molecular states as quantum beats in the dynamical overlap function.

Model.—Consider an ion of mass m immersed in a BEC of atoms of mass m_B. The Hamiltonian is

$$\hat{H} = \sum_{\mathbf{k}} \left(\frac{\mathbf{k}^2}{2m} \hat{a}^\dagger_{\mathbf{k}} \hat{a}_{\mathbf{k}} + \frac{\mathbf{k}^2}{2m_B} \hat{b}^\dagger_{\mathbf{k}} \hat{b}_{\mathbf{k}} \right) + \frac{g_B}{2} \sum_{\mathbf{k},\mathbf{k}',\mathbf{q}} \hat{b}^\dagger_{\mathbf{k}+\mathbf{q}} \hat{b}^\dagger_{\mathbf{k}'-\mathbf{q}} \hat{b}_{\mathbf{k}'} \hat{b}_{\mathbf{k}} + \sum_{\mathbf{k},\mathbf{k}',\mathbf{q}} V(\mathbf{q}) \hat{a}^\dagger_{\mathbf{k}'-\mathbf{q}} \hat{a}_{\mathbf{k}'} \hat{b}^\dagger_{\mathbf{k}+\mathbf{q}} \hat{b}_{\mathbf{k}}, \tag{1}$$

where $\hat{a}^\dagger_{\mathbf{k}}$ and $\hat{b}^\dagger_{\mathbf{k}}$ creates an ion and a boson, respectively, with momentum $\mathbf{k}$. We describe the BEC of density n_0

using Bogoliubov theory giving the dispersion $E_{\mathbf{k}} = \sqrt{\epsilon_{\mathbf{k}}^2 + 2n_0 g_B \epsilon_{\mathbf{k}}}$ with $\epsilon_{\mathbf{k}} = \mathbf{k}^2/2m_B$ and $g_B = 4\pi a_B/m_B$ with a_B the atom-atom scattering length. The atom-ion interaction is $V(\mathbf{k})$, and we use units where the system volume and $\hbar$ are unity.

In real space, the atom-ion interaction has the long-range asymptotic form $V(\mathbf{r}) \sim -\alpha/r^4$, where α is proportional to the polarizability of the atoms [29]. A characteristic length scale of the interaction is therefore $r_{\text{ion}} = \sqrt{2m_r\alpha}$ with $m_r^{-1} = m^{-1} + m_B^{-1}$, and using the polarizability of atoms like ^{87}Rb and ^{23}Na this gives $r_{\text{ion}} \sim \mathcal{O}(10^2)$ nm [26]. This is of the same order as the average interparticle distance for a typical BEC with density $n_0 \sim 10^{14}$ cm^{-3}, and it is therefore crucial to include the asymptotic form of $V(\mathbf{r})$ in our analysis. To do this, we use the effective interaction [30]

$$V(r) = -\frac{\alpha}{(r^2+b^2)^2}\frac{r^2-c^2}{r^2+c^2}, \tag{2}$$

where the parameter c establishes a repulsive barrier such that the potential is repulsive (attractive) for $c < r (c > r)$, while b is related to the depth of the potential. We have $V(0) = \alpha/b^4$, which is large compared to any other relevant energy in order to mimic the strong repulsion when the electron clouds of the atom and the ion overlap. In the inset of Fig. 1, we plot $V(r)$ in units of $\mathcal{E}_{\text{ion}} = 1/2m_r r_{\text{ion}}^2$ for two different values of b. For concreteness, here and in the rest of the Letter we consider a ^{87}Rb$^+$ ion in a ^{87}Rb BEC, which can be created by photoionization. In this case, $c = 0.0023 r_{\text{ion}}$ in Eq. (2), $m = m_B$.

Ion-atom scattering.—In Fig. 1, the atom-ion scattering length a, obtained by solving the zero energy s-wave Schrödinger equation with the potential $V(r)$, is plotted as a function of b. It exhibits several divergencies, which correspond to the emergence of two-body bound states. The first bound state appears for $b/r_{\text{ion}} \simeq 0.58$, and more bound states appear as the atom-ion potential becomes deeper with decreasing b.

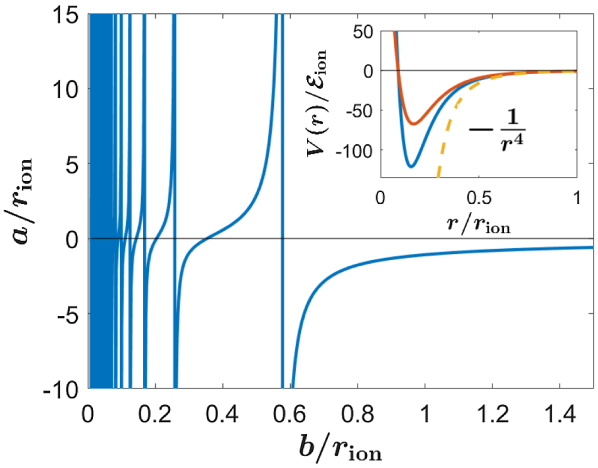

FIG. 1. Atom-ion s-wave scattering length a as a function of b. Inset: atom-ion potential for $b/r_{\text{ion}} = 0.3$ and 0.35.

A key point is that when the range of the interaction r_{ion} is of the order of or larger than the interparticle distance, i.e., $r_{\text{ion}} \gtrsim n_0^{-1/3}$, we cannot employ the usual short-range pseudopotential, which has been successfully used to describe neutral atomic gases. Instead, we need to retain the full interaction Eq. (2) in our analysis of this strongly interacting many-body system.

Polarons.—We start by analyzing arguably the most interesting case, i.e., the high density regime. To account for the strength and range of the ion-atom interaction, which may lead to correlations involving many bosons around the ion, we use a coherent state variational ansatz

$$|\Psi(t)\rangle = e^{-i\phi(t)} e^{\sum_{\mathbf{k}} [\gamma_{\mathbf{k}}(t)\hat{\beta}_{\mathbf{k}}^\dagger - \gamma_{\mathbf{k}}^*(t)\hat{\beta}_{\mathbf{k}}]} |\Psi(0)\rangle, \tag{3}$$

that allows the ion to be dressed by an infinite amount of Bogoliubov modes. Here, $\hat{\beta}_{\mathbf{k}}^\dagger = u_{\mathbf{k}}\hat{b}_{\mathbf{k}}^\dagger + v_{\mathbf{k}}\hat{b}_{-\mathbf{k}}$ creates a Bogoliubov mode with momentum $\mathbf{k}$ and energy $E_{\mathbf{k}}$, and $\phi(t)$ and $\gamma_{\mathbf{k}}(t)$ are the variational parameters [31]. The initial state $|\Psi(0)\rangle = \hat{a}_{\mathbf{k}=0}^\dagger |\text{BEC}\rangle$ corresponds to the injection of a zero momentum ion in the BEC. We determine the dynamical overlap $S(t) = \langle\Psi(0)|\Psi(t)\rangle = e^{-i\phi(t)} e^{-1/2\sum_{\mathbf{k}} |\gamma_{\mathbf{k}}|^2}$. The impurity spectral function can then be obtained by a Fourier transform $A(\omega) = \text{Re}\int_0^\infty S(t) e^{i\omega t} dt/\pi$ [31,34].

In Fig. 2 (top), we plot the spectral function for the density $n_0 r_{\text{ion}}^3 = 1$ and zero temperature as a function of b and the corresponding scattering length a. For large b meaning weak coupling $1/k_n a \ll -1$ with $k_n^3/6\pi^2 = n_0$, there is a well-defined quasiparticle with mean-field energy $E = 2\pi a n_0/m_r$. Its energy decreases with decreasing b (increasing $1/k_n a$) corresponding to an increasing depth of the potential, and the mean-field expression eventually breaks down. This quasiparticle is the attractive Bose polaron for the ion in direct analogy with what is observed for neutral impurities [35–38]. Since we have added a small imaginary part to the frequency for numerical reasons, its quasiparticle peak becomes indistinguishable from the many-body continuum starting at energies just above [39]. The attractive polaron remains a stable ground state with decreasing b but with a very small residue.

To further analyze the nature of the polaron, we use a thermodynamic argument to calculate the number of atoms ΔN in the dressing cloud around the ion as [26,40]

$$\Delta N = -\left(\frac{\partial \mu_I}{\partial n_0}\right)\left(\frac{\partial n_0}{\partial \mu_B}\right)_{n_I=0} = -\left(\frac{\partial \mu_I}{\partial \mu_B}\right)_{n_I=0}, \tag{4}$$

where μ_I is the energy change when the ion is added to the BEC, $\mu_B = g_B n_0$ is the chemical potential of the atoms, and n_I is the ion density, which is zero for a single ion. For a given many-body state with energy $\mathcal{E}_j$ obtained from

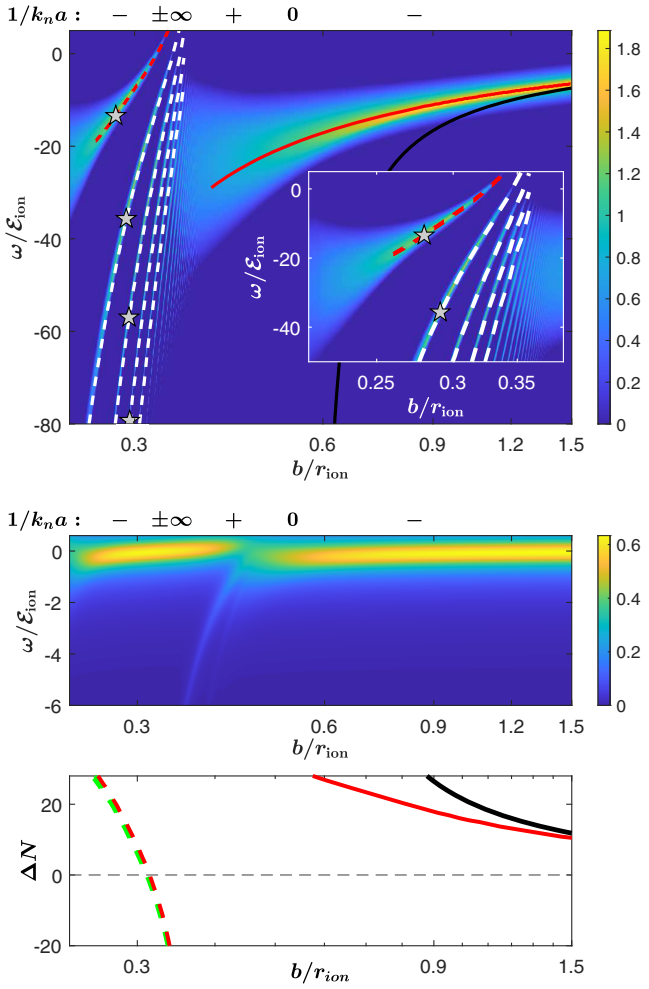

FIG. 2. Zero momentum ion spectral function $A(\omega)$ as a function of the potential parameter b and the corresponding scattering length a for $n_0 r_{\rm ion}^3 = 1$ (top) and $n_0 r_{\rm ion}^3 = 0.01$ (middle). The black line is the mean-field energy, the red line is the ladder approximation for the attractive polaron present for $b/r_{\rm ion} \gtrsim 0.5$, the red dashed line the repulsive polaron present for $b/r_{\rm ion} \lesssim 0.34$, and the white lines are the molecular states obtained from the Bethe-Salpeter equation. The stars ⋆ signify the breakdown of the Bogoliubov approximation. Bottom: number of atoms in the dressing cloud with the same color coding as the top panel, except the white molecular lines, which are represented as green lines. In the top panel, we take the logarithm to the spectral function, which visually makes the width appear larger. Middle panel is in linear scale.

Eq. (3), we set $\mu_I = \mathcal{E}_j$ in Eq. (4) and calculate ΔN by numerical differentiation.

In Fig. 2 (bottom), we see that number of bosons in the dressing cloud around the ion in the polaronic state is quite large reflecting the strength and range of the atom-ion interaction. In the weak coupling limit $b/r_{\rm ion} \gg 1$, we recover the mean-field result $\Delta N = -a/a_B$ [26].

Figure 2 (top) furthermore shows that a number of new states emerge in the regime $b/r_{\rm ion} < 0.58$ where the interaction supports a two-body bound state. We have $a > 0$ for $0.58 > b/r_{\rm ion} > 0.35$ and $a \leq 0$ for $0.35 \geq b/r_{\rm ion} > 0.26$ where another bound state emerges, see Fig. 1. Consider first the branch with the highest energy emerging for $b/r_{\rm ion} \simeq 0.34 \Rightarrow 1/k_n a \simeq -1.45$, shown by a red dashed line. Its energy ε_P is larger than zero for $b/r_{\rm ion} \gtrsim 0.32$, and in addition the number of particles ΔN in its dressing cloud is negative as shown in the bottom panel. From this we conclude that it is a repulsive polaron. Its energy becomes negative for $b/r_{\rm ion} \lesssim 0.32$ where $\Delta N > 0$ showing that it smoothly evolves into an attractive polaron with increasing depth of the ion-atom interaction potential. This is qualitatively different from the case of a neutral impurity with a short-range interaction, where there is no attractive polaron when there is a bound state.

Molecular ions.—We now turn our attention to the low energy states emerging together with the repulsive polaron at $b/r_{\rm ion} \lesssim 0.34$ in Fig. 2 (top) and seen more clearly in the inset. They are molecular ions arising from the binding of $1, 2, \ldots$ bosons to the ion. To demonstrate this, we use the Bethe-Salpeter equation, which provides a general framework for analyzing bound states in a many-body environment. Consider the scattering matrix between an ion with momentum/energy $k_1 = (\mathbf{k}_1, i\omega_1)$ and an atom with momentum/energy $k_2 = (\mathbf{k}_2, i\omega_2)$. In the ladder approximation, it obeys the Bethe-Salpeter equation [31]

$$\Gamma(\mathbf{k}_1, \mathbf{k}_2, \mathbf{q}; i\omega_1 + i\omega_2) = V(\mathbf{q}) - \sum_{q'} V(\mathbf{q}') G_{11}(k_2 - q') \times G(k_1 + q') \Gamma(\mathbf{k}_1 + \mathbf{q}', \mathbf{k}_2 - \mathbf{q}', \mathbf{q} - \mathbf{q}'; i\omega_1 + i\omega_2), \tag{5}$$

where $\mathbf{q}$ is the momentum transfer, $G(k) = 1/(i\omega - \mathbf{k}^2/2m)$ is the ion Green's function, and $G_{11}(k) = u_{\mathbf{k}}^2/(i\omega - E_{\mathbf{k}}) - v_{\mathbf{k}}^2/(i\omega + E_{\mathbf{k}})$ is the normal (as opposed to anomalous) BEC Green's function for the atoms. The sum $\sum_{q'} \equiv T \sum_{i\omega} \int d^3q/(2\pi)^3$ is both over momenta $\mathbf{q}$ and Matsubara frequencies $i\omega$, and we analytically continue $i\omega \to \omega + i0_+$ as usual. Because of the long range of the atom-ion potential, it is essential to retain its full momentum dependence in Eq. (5), in contrast to the usual case of a short-range interaction between neutral atoms.

The ion self-energy $\Sigma(\mathbf{k}, \omega) = n_0 \Gamma(\mathbf{k}, 0, 0; \omega)$ describes the scattering of a single atom out of the BEC, and the quasiparticle energy is obtained by solving $\varepsilon_{P,\mathbf{k}} = k^2/2m + \Sigma(\mathbf{k}, \varepsilon_{P,\mathbf{k}})$. The resulting ladder approximation has successfully been applied to explain experimental results for neutral impurities in a BEC forming Bose polarons [35–38,41]. In the present case it yields the red line in Fig. 2 (top), which agrees very well with the variational result for the attractive polaron stable, whereas it fails to capture the lower lying states.

This can, however, be addressed by noting that a pole of the zero momentum scattering matrix gives the energy of a bound state. Thus, replacing in Eq. (5) the bare ion Green's function with the polaron Green's function $G_j(k) = 1/(i\omega - \varepsilon_P - \mathbf{k}^2/2m)$ will give the energy of a dimer consisting of an atom bound to the polaron. This yields the top white dashed line in Fig. 2 (top). The excellent agreement with the variational ansatz shows that this state indeed arises from the binding of an atom to the polaron. We perform this procedure recursively by calculating the scattering matrix between this new molecular state and an atom, which then yields the second white line below the attractive polaron in Fig. 2 and so on. Note that we have used unit residues of all propagators in Eq. (5), which physically corresponds to assuming that the molecules interact with the ion in the same way as bare atoms. This is obviously an approximation, but since the energies obtained from this procedure agree very well with those from the variational ansatz, we conclude that these branches indeed involve the binding of one, two, … atoms to the ion. In the following, we refer for brevity to these states as molecular ions although they do have a nonzero quasiparticle residue as is evident from Fig. 2. We note that dimer states consisting of one atom bound to the ion have recently been observed [21], and our prediction of molecular states involving more atoms is consistent with earlier results based on different methods [25–28].

Note that these molecules are stable only for b significantly smaller than $b/r_{\mathrm{ion}} = 0.58$ where the two-body atom-ion state emerges. Hence, many-body effects destabilize the binding of atoms to the ion as compared to the vacuum case. The molecules are stable for $a > 0$ and $a < 0$ as opposed to the case of a short-range interaction, where similar states are predicted to exist only for $a < 0$ [42], again showing the qualitative differences between a charged and a neutral impurity.

The binding of additional atoms to the ion will eventually be halted by the repulsion between them giving a positive energy $\sim a_B \Delta N^2$. While this effect is not included in our theory, we can estimate when it becomes important by calculating the gas factor of the dressing cloud $\sqrt{n_{\mathrm{cl}} a_B^3}$. Here, $n_{\mathrm{cl}} = \Delta N/\bar{r}^3$ is the average density of atoms in the dressing cloud with $\bar{r} = [\int d^3 r r^2 |\phi(\mathbf{r})|^2]^{1/2}$ the spatial size of the molecule with wave function $\phi(\mathbf{r})$. As explicitly shown in the Supplemental Material [31], the size of the molecular states is $\sim r_{\mathrm{ion}}$ and decreases as they become increasingly bound. This is around 3 orders of magnitude larger than the ground state size of Rb_2^+ [43], consistent with their binding energy being much smaller. The $\star$'s in Fig. 2 indicate when the gas factor of a given molecular state becomes larger than 0.1. A reliable description of the region below the stars requires one to go beyond Bogoliubov theory.

The basic physics of the binding of bosons to the ion can be captured using the Hamiltonian

$$\hat{H}_s = \sum_{l=0}^{\infty} \{[\varepsilon_P + \varepsilon_B(l-1)]\hat{c}_l^\dagger \hat{c}_l + g\sqrt{n_0}\hat{c}_{l+1}^\dagger \hat{c}_l + \mathrm{H.c.}\}. \quad (6)$$

Here, $\hat{c}_l$ creates a state with l bosons bound to the polaron, $\varepsilon_B < 0$ is the energy released by the binding of a boson, and $g\sqrt{n_0}$ is the matrix element for this process. Note that this is proportional to $\sqrt{n_0}$ since the boson is taken from the BEC with density n_0. This also means that we can suppress the momentum since this is zero for all states. The model is easily solved giving a continued fraction form of the zero momentum ion Green's function

$$G(\omega)^{-1} = \omega - \varepsilon_P - \cfrac{g^2 n_0}{\omega - \varepsilon_B - \cfrac{g^2 n_0}{\omega - 2\varepsilon_B - \cfrac{g^2 n_0}{\omega - 3\varepsilon_B - \ldots}}}. \quad (7)$$

For $g^2 n_0/\varepsilon_B^2 \ll 1$, the highest energy pole is $\simeq \varepsilon_P$ corresponding to the repulsive polaron and there is an infinite ladder of poles with energies $\simeq \varepsilon_P - l\varepsilon_B$ corresponding to states with $l = 1, 2, \ldots$ bosons bound to the ion. The residue of these states is $(g^2 n_0/\varepsilon_B^2)^l \propto n_0^l$ reflecting that they involve l bosons taken from the BEC. This scaling explains the decreasing spectral weight of the deeper molecular lines seen Fig. 2 (top).

It also means that the relative spectral weight of the different lines depends on the BEC density. This is illustrated in Fig. 2 (middle), which shows the ion spectral function for $n_0 r_{\mathrm{ion}}^3 = 0.01$. We see that only two states with significant spectral weight emerge for $b/r_{\mathrm{ion}} < 0.58$ when the atom-ion potential supports a bound state: the new polaron and the highest molecular state with one boson bound to the ion. Since the ground state remains the attractive polaron, this is consistent with the finding that for a static ion in the dilute limit, there are $2\nu_s + 1$ solutions to the Gross-Pitaevskii equation where ν_s is the number of two-body bound states of the atom-ion interaction potential [26,44]. The small spectral weight of the bound states involving more than one boson also means that they are quite sensitive to additional damping.

Dynamics.—We finally investigate the quantum dynamics after a zero momentum ion is injected in the BEC. The overlap $S(t) = \langle \Psi(0)|\Psi(t)\rangle$ is plotted in Fig. 3. For $b/r_{\mathrm{ion}} = 2$, we have $|S(t)| \to Z$ for $t \to \infty$ where Z is the quasiparticle residue of the attractive polaron [42,45–47]. For $b/r_{\mathrm{ion}} = 0.5$ on the other hand, $S(t)$ decreases monotonically to zero since the quasiparticle has a vanishingly small residue, see Fig. 2 (top). In the right panel of Fig. 3, we plot $S(t)$ when the molecular states are present. For $b/r_{\mathrm{ion}} = 0.3$ (orange), $S(t)$ oscillates with an almost constant amplitude after an initial decay. These oscillations arise from a coherent population of the molecular states and the polaron, see Fig. 2 (top). For $b/r_{\mathrm{ion}} = 0.25$ (blue) on the other hand, the polaron is

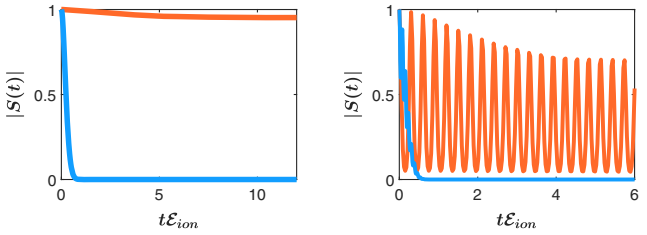

FIG. 3. Left: $|S(t)|$ is shown for $b/r_{\mathrm{ion}} = 2$ (orange) and $b/r_{\mathrm{ion}} = 0.5$ (blue). Right: $|S(t)|$ for $b/r_{\mathrm{ion}} = 0.3$ (orange) and $b/r_{\mathrm{ion}} = 0.25$ (blue). We take $n_0 r_{\mathrm{ion}}^3 = 1$.

strongly damped giving rise to decoherence and $S(t)$ therefore decays monotonically to zero, see Fig. 2 (top).

Figure 3 shows that the many-body timescale is $\tau_{\mathrm{ion}} \approx 1/\mathcal{E}_{\mathrm{ion}}$. For $b/r_{\mathrm{ion}} = 0.25$ and $r_{\mathrm{ion}} = 100$ nm it is of the order of $\tau_{\mathrm{ion}} \approx 13.55$ μs. This should be compared to the three-body recombination time $\tau_{3\mathrm{B}} = 1/K_3 n_0^2$. Taking $K_3 \approx 3.3$–6×10^{25} cm^6/s [20,48] and $n_0 = 10^{14}$ cm^{-3} for a typical BEC yields $\tau_{3\mathrm{B}} \approx 160$–$300$ μs. Also, the time resolution for state-of-the-art hybrid ion-atom experiments is ≈10 ns. We conclude that the many-body phenomena described here should be observable before three-body decay sets in.

Conclusions and outlook.—We studied the static and dynamical properties of a mobile ion in a BEC. The long-range nature of the atom-ion interaction was shown to result in a rich spectrum with several quasiparticle and molecular ions. We demonstrated that the quantum dynamics after a quench where the ion is injected into the BEC is characterized by coherent oscillations between the different states as well as decay. Our work demonstrates the diverse and exciting physics that can be realized in ion-atom systems and may serve as a guide as well as motivate future investigations into these hybrid systems. In particular, dimer states consisting of one atom bound to the ion have recently been observed, and it would be very interesting to extend this experimental search to the predicted deeper lying larger molecular ions preferably using a high density BEC [21]. The long-range nature of the interaction furthermore makes ion-atom systems well suited for exploring angular momentum exchange of the molecules with the surroundings [49–52]. Radio-frequency and Ramsey spectroscopy have been used to measure the spectral function and the dynamics for neutral impurities [35–38,46,53,54], and analogous probes for charged impurities would be highly useful.

We thank P. Massignan for very useful comments, and T. Pohl and K. Mølmer for discussions. We acknowledge financial support from the Villum Foundation, the Independent Research Fund Denmark-Natural Sciences via Grant No. DFF -8021-00233B, and the U.S. Army CCDC Atlantic Basic and Applied Research via Grant No. W911NF-19-1-0403.

[1] I. Bloch, J. Dalibard, and W. Zwerger, Many-body physics with ultracold gases, Rev. Mod. Phys. **80**, 885 (2008).
[2] I. Bloch, J. Dalibard, and S. Nascimbene, Quantum simulations with ultracold quantum gases, Nat. Phys. **8**, 267 (2012).
[3] E. J. Yarmchuk, M. J. V. Gordon, and R. E. Packard, Observation of Stationary Vortex Arrays in Rotating Superfluid Helium, Phys. Rev. Lett. **43**, 214 (1979).
[4] L. Meyer and F. Reif, Mobilities of He ions in liquid helium, Phys. Rev. **110**, 279 (1958).
[5] K. R. Atkins, Ions in liquid helium, Phys. Rev. **116**, 1339 (1959).
[6] E. P. Gross, Motion of foreign bodies in boson systems, Ann. Phys. (N.Y.) **19**, 234 (1962).
[7] A. I. Ahonen, J. Kokko, O. V. Lounasmaa, M. A. Paalanen, R. C. Richardson, W. Schoepe, and Y. Takano, Mobility of Negative Ions in Superfluid ^{3}He, Phys. Rev. Lett. **37**, 511 (1976).
[8] Paul D. Roach, J. B. Ketterson, and Pat R. Roach, Mobility of Positive and Negative Ions in Superfluid ^{3}He, Phys. Rev. Lett. **39**, 626 (1977).
[9] A. I. Ahonen, J. Kokko, M. A. Paalanen, R. C. Richardson, W. Schoepe, and Y. Takano, Negative ion motion in normal and superfluid ^{3}He, J. Low Temp. Phys. **30**, 205 (1978).
[10] M. Salomaa, C. J. Pethick, and Gordon Baym, Mobility Tensor of the Electron Bubble in Superfluid ^{3}He-*a*, Phys. Rev. Lett. **44**, 998 (1980).
[11] G. Baym, C. J. Pethick, and M. Salomaa, Mobility of negative ions in superfluid ^{3}He-b, J. Low Temp. Phys. **36**, 431 (1979).
[12] A. T. Grier, M. Cetina, F. Oručević, and V. Vuletić, Observation of Cold Collisions between Trapped Ions and Trapped Atoms, Phys. Rev. Lett. **102**, 223201 (2009).
[13] C. Zipkes, S. Palzer, C. Sias, and M. Köhl, A trapped single ion inside a Bose-Einstein condensate, Nature (London) **464**, 388 (2010).
[14] A.Härter, A. Krükow, A. Brunner, W. Schnitzler, S. Schmid, and J. H. Denschlag, Single Ion as a Three-Body Reaction Center in an Ultracold Atomic Gas, Phys. Rev. Lett. **109**, 123201 (2012).
[15] L. Ratschbacher, C. Zipkes, C. Sias, and M. Köhl, Controlling chemical reactions of a single particle, Nat. Phys. **8**, 649 (2012).
[16] K. S. Kleinbach, F. Engel, T. Dieterle, R. Löw, T. Pfau, and F. Meinert, Ionic Impurity in a Bose-Einstein Condensate at Submicrokelvin Temperatures, Phys. Rev. Lett. **120**, 193401 (2018).
[17] T. Sikorsky, Z. Meir, R. Ben-shlomi, N. Akerman, and R. Ozeri, Spin-controlled atom-ion chemistry, Nat. Commun. **9**, 920 (2018).
[18] T. Feldker, H. Fürst, H. Hirzler, N. V. Ewald, M. Mazzanti, D. Wiater, M. Tomza, and R. Gerritsma, Buffer gas cooling of a trapped ion to the quantum regime, Nat. Phys. **16**, 413 (2020).
[19] J. Schmidt, P. Weckesser, F. Thielemann, T. Schaetz, and L. Karpa, Optical Traps for Sympathetic Cooling of Ions with Ultracold Neutral Atoms, Phys. Rev. Lett. **124**, 053402 (2020).
[20] T. Dieterle, M. Berngruber, C. Hölzl, R. Löw, K. Jachymski, T. Pfau, and F. Meinert, Transport of a Single Cold Ion

Immersed in a Bose-Einstein Condensate, Phys. Rev. Lett. **126**, 033401 (2021).
[21] T. Dieterle, M. Berngruber, C. Hölzl, R. Löw, K. Jachymski, T. Pfau, and F. Meinert, Inelastic collision dynamics of a single cold ion immersed in a Bose-Einstein condensate, Phys. Rev. A **102**, 041301(R) (2020).
[22] W. Casteels, J. Tempere, and J. T. Devreese, Polaronic properties of an ion in a Bose-Einstein condensate in the strong-coupling limit, J. Low Temp. Phys. **162**, 266 (2011).
[23] B. Gao, Universal Properties in Ultracold Ion-Atom Interactions, Phys. Rev. Lett. **104**, 213201 (2010).
[24] A. Krükow, A. Mohammadi, A. Härter, J. H. Denschlag, J. Pérez-Ríos, and C. H. Greene, Energy Scaling of Cold Atom-Atom-Ion Three-Body Recombination, Phys. Rev. Lett. **116**, 193201 (2016).
[25] R. Côté, V. Kharchenko, and M. D. Lukin, Mesoscopic Molecular Ions in Bose-Einstein Condensates, Phys. Rev. Lett. **89**, 093001 (2002).
[26] P. Massignan, C. J. Pethick, and H. Smith, Static properties of positive ions in atomic Bose-Einstein condensates, Phys. Rev. A **71**, 023606 (2005).
[27] J. M. Schurer, A. Negretti, and P. Schmelcher, Unraveling the Structure of Ultracold Mesoscopic Collinear Molecular Ions, Phys. Rev. Lett. **119**, 063001 (2017).
[28] G. E. Astrakharchik, L. A. Peña Ardila, R. Schmidt, K. Jachymski, and A. Negretti, Ionic polaron in a Bose-Einstein condensate, Commun. Phys. **4**, 94 (2021).
[29] M. Tomza, K. Jachymski, R. Gerritsma, A. Negretti, T. Calarco, Z. Idziaszek, and P. S. Julienne, Cold hybrid ion-atom systems, Rev. Mod. Phys. **91**, 035001 (2019).
[30] M. Krych and Z. Idziaszek, Description of ion motion in a paul trap immersed in a cold atomic gas, Phys. Rev. A **91**, 023430 (2015).
[31] See Supplemental Material at http://link.aps.org/supplemental/10.1103/PhysRevLett.126.243001, which includes Refs. [32,33], for equations of motions, numerical procedures, and the Bethe-Salpeter approach for molecular states.
[32] David Dzsotjan, Richard Schmidt, and Michael Fleischhauer, Dynamical Variational Approach to Bose Polarons at Finite Temperatures, Phys. Rev. Lett. **124**, 223401 (2020).
[33] H. Dishan, Phase error in fast fourier transform analysis, Mech. Syst. Signal Process. **9**, 113 (1995).
[34] M. Knap, A. Shashi, Y. Nishida, A. Imambekov, D. A. Abanin, and E. Demler, Time-Dependent Impurity in Ultracold Fermions: Orthogonality Catastrophe and Beyond, Phys. Rev. X **2**, 041020 (2012).
[35] N. B. Jørgensen, L. Wacker, K. T. Skalmstang, M. M. Parish, J. Levinsen, R. S. Christensen, G. M. Bruun, and J. J. Arlt, Observation of Attractive and Repulsive Polarons in a Bose-Einstein Condensate, Phys. Rev. Lett. **117**, 055302 (2016).
[36] M.-G. Hu, M. J. Van de Graaff, D. Kedar, J. P. Corson, E. A. Cornell, and D. S. Jin, Bose Polarons in the Strongly Interacting Regime, Phys. Rev. Lett. **117**, 055301 (2016).
[37] L. A. Peña Ardila, N. B. Jørgensen, T. Pohl, S. Giorgini, G. M. Bruun, and J. J. Arlt, Analyzing a Bose polaron across resonant interactions, Phys. Rev. A **99**, 063607 (2019).
[38] Z. Z. Yan, Y. Ni, C. Robens, and M. W. Zwierlein, Bose polarons near quantum criticality, Science **368**, 190 (2020).
[39] In the top panel of Fig. 2, we take the logarithm to the spectral function, which visually makes the width appear larger.
[40] P. Massignan and G. M. Bruun, Repulsive polarons and itinerant ferromagnetism in strongly polarized fermi gases, Eur. Phys. J. D **65**, 83 (2011).
[41] S. P. Rath and R. Schmidt, Field-theoretical study of the Bose polaron, Phys. Rev. A **88**, 053632 (2013).
[42] Y. E. Shchadilova, R. Schmidt, F. Grusdt, and E. Demler, Quantum Dynamics of Ultracold Bose Polarons, Phys. Rev. Lett. **117**, 113002 (2016).
[43] F. Spiegelmann, D. Pavolini, and J. P. Daudey, Theoretical study of the excited states of the heavier alkali dimers. II. The rb2 molecule, J. Phys. B **22**, 2465 (1989).
[44] We thank P. Massignan for pointing this result out for us.
[45] K. K. Nielsen, L. A. Peña Ardila, G. M. Bruun, and T. Pohl, Critical slowdown of nonequilibrium polaron dynamics, New J. Phys. **21**, 043014 (2019).
[46] M. Cetina, M. Jag, R. S. Lous, I. Fritsche, J. T. M. Walraven, R. Grimm, J. Levinsen, M. M. Parish, R. Schmidt, M. Knap, and E. Demler, Ultrafast many-body interferometry of impurities coupled to a fermi sea, Science **354**, 96 (2016).
[47] M. M. Parish and J. Levinsen, Quantum dynamics of impurities coupled to a Fermi sea, Phys. Rev. B **94**, 184303 (2016).
[48] A. Härter, A. Krükow, A. Brunner, W. Schnitzler, S. Schmid, and J. H. Denschlag, Single Ion as a Three-Body Reaction Center in an Ultracold Atomic Gas, Phys. Rev. Lett. **109**, 123201 (2012).
[49] R. Schmidt and M. Lemeshko, Rotation of Quantum Impurities in the Presence of a Many-Body Environment, Phys. Rev. Lett. **114**, 203001 (2015).
[50] C. P. Koch, M. Lemeshko, and D. Sugny, Quantum control of molecular rotation, Rev. Mod. Phys. **91**, 035005 (2019).
[51] J. L. Hansen, J. J. Omiste, J. H. Nielsen, D. Pentlehner, J. Kpper, R. Gonzlez-Frez, and H. Stapelfeldt, Mixed-field orientation of molecules without rotational symmetry, J. Chem. Phys. **139**, 234313 (2013).
[52] B. Shepperson, A. A. Søndergaard, L. Christiansen, J. Kaczmarczyk, R. E. Zillich, M. Lemeshko, and H. Stapelfeldt, Laser-Induced Rotation of Iodine Molecules in Helium Nanodroplets: Revivals and Breaking Free, Phys. Rev. Lett. **118**, 203203 (2017).
[53] M. Cetina, M. Jag, R. S. Lous, J. T. M. Walraven, R. Grimm, R. S. Christensen, and G. M. Bruun, Decoherence of Impurities in a Fermi Sea of Ultracold Atoms, Phys. Rev. Lett. **115**, 135302 (2015).
[54] M. G. Skou, T. G. Skov, N. B. Jørgensen, K. K. Nielsen, A. Camacho-Guardian, T. Pohl, G. M. Bruun, and J. J. Arlt, Non-equilibrium quantum dynamics and formation of the Bose polaron, Nat. Phys. **17**, 731 (2021).